This is a repository copy of *Polariton lasing in AlGaN microring with GaN/AlGaN quantum wells*.

White Rose Research Online URL for this paper:
https://eprints.whiterose.ac.uk/196623/

Version: Published Version

Article:
Delphan, A. orcid.org/0000-0002-1197-7736, Makhonin, M.N. orcid.org/0000-0003-0457-9024, Isoniemi, T. orcid.org/0000-0003-0238-1006 et al. (7 more authors) (2023) Polariton lasing in AlGaN microring with GaN/AlGaN quantum wells. APL Photonics, 8 (2). 021302. ISSN 2378-0967

https://doi.org/10.1063/5.0132170

Reuse
This article is distributed under the terms of the Creative Commons Attribution (CC BY) licence. This licence allows you to distribute, remix, tweak, and build upon the work, even commercially, as long as you credit the authors for the original work. More information and the full terms of the licence here: https://creativecommons.org/licenses/

Takedown
If you consider content in White Rose Research Online to be in breach of UK law, please notify us by emailing eprints@whiterose.ac.uk including the URL of the record and the reason for the withdrawal request.

eprints@whiterose.ac.uk
https://eprints.whiterose.ac.uk/

APL Photonics

Polariton lasing in AlGaN microring with GaN/AlGaN quantum wells

Cite as: APL Photonics **8**, 021302 (2023); https://doi.org/10.1063/5.0132170
Submitted: 27 October 2022 • Accepted: 09 January 2023 • Accepted Manuscript Online: 09 January 2023 • Published Online: 02 February 2023

Anthonin Delphan, Maxim N. Makhonin, Tommi Isoniemi, et al.

View Online Export Citation CrossMark

ARTICLES YOU MAY BE INTERESTED IN

High-dimensional spatial mode sorting and optical circuit design using multi-plane light conversion
APL Photonics **8**, 026101 (2023); https://doi.org/10.1063/5.0128431

High-speed uni-traveling-carrier photodiodes on silicon nitride
APL Photonics **8**, 016104 (2023); https://doi.org/10.1063/5.0119244

Efficient chip-based optical parametric oscillators from 590 to 1150 nm
APL Photonics **7**, 121301 (2022); https://doi.org/10.1063/5.0117691

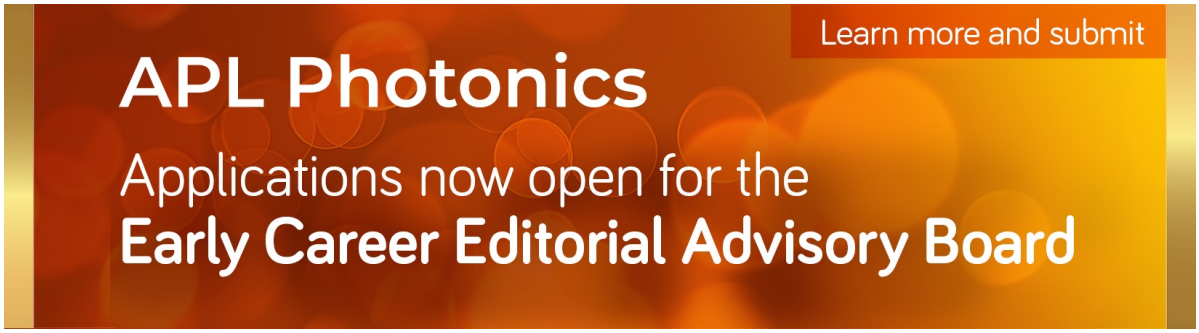

AIP Publishing

© 2023 Author(s).

Polariton lasing in AlGaN microring with GaN/AlGaN quantum wells

Cite as: APL Photon. 8, 021302 (2023); doi: 10.1063/5.0132170
Submitted: 27 October 2022 • Accepted: 9 January 2023 •
Published Online: 2 February 2023

View Online Export Citation CrossMark

Anthonin Delphan,[1] Maxim N. Makhonin,[1] Tommi Isoniemi,[1] Paul M. Walker,[1] Maurice S. Skolnick,[1] Dmitry N. Krizhanovskii,[1] Dmitry V. Skryabin,[2] Jean-François Carlin,[3] Nicolas Grandjean,[3] and Raphaël Butté[3,a)]

AFFILIATIONS

[1] Department of Physics and Astronomy, University of Sheffield, Sheffield S3 7RH, United Kingdom
[2] Department of Physics, University of Bath, Claverton Down, Bath BA2 7AY, United Kingdom
[3] Institute of Physics, École Polytechnique Fédérale de Lausanne (EPFL), CH-1015 Lausanne, Switzerland

[a)] Author to whom correspondence should be addressed: raphael.butte@epfl.ch

ABSTRACT

Microcavity polaritons are strongly interacting hybrid light–matter quasiparticles, which are promising for the development of novel light sources and active photonic devices. Here, we report polariton lasing in the UV spectral range in microring resonators based on GaN/AlGaN slab waveguides, with experiments carried out from 4 K up to room temperature. Stimulated polariton relaxation into multiple ring resonator modes is observed, which exhibit threshold-like dependence of the emission intensity with pulse energy. The strong exciton-photon coupling regime is confirmed by the significant reduction of the free spectral range with energy and the blueshift of the exciton–like modes with increasing pulse energy. Importantly, the exciton emission shows no broadening with power, further confirming that lasing is observed at electron–hole densities well below the Mott transition. Overall, our work paves the way toward the development of novel UV devices based on the high-speed slab waveguide polariton geometry operating up to room temperature with the potential to be integrated into complex photonic circuits.

© 2023 Author(s). All article content, except where otherwise noted, is licensed under a Creative Commons Attribution (CC BY) license (http://creativecommons.org/licenses/by/4.0/). https://doi.org/10.1063/5.0132170

Microcavity polaritons are hybrid light–matter quasiparticles, arising from strong exciton–photon coupling in semiconductor photonic structures. They have attracted significant attention in the last 15 years with a number of fundamental effects observed such as polariton condensation[1] and lasing,[2] superfluidity,[3] solitons,[4] polariton blockade,[5] and single polariton nonlinearity,[6] to name just a few, which are enabled by giant polariton interactions. Interacting polaritons are highly promising for the development of novel quantum light sources, photonic nonlinear simulators,[7] logic gates, and quantum optical signal processing.[8]

Polariton lasing, the coherent light emission from polariton condensates, provides several advantages over standard photonic lasing, including operation without population inversion with a threshold lower than that in conventional semiconductor lasers.[9] It has been demonstrated via optical[2,10] and electrical pumping.[11] Room temperature (RT) operation has been reported in structures based on wide bandgap semiconductors[10,12,13] enabled by their large exciton binding energy. Polariton lasing has been mainly studied in planar semiconductor microcavities (MCs) made of two Bragg mirrors, which are challenging to fabricate. On the other hand, polaritons have also been investigated in the slab waveguide (WG) geometry,[14,15] where photonic confinement in the vertical direction arises from total internal reflection (TIR). The main advantages of the WG geometry over MCs are low disorder due to thinner and simpler structures and the high polariton speed, enabling long propagation distances up to several hundreds of μm, which makes this system favorable for the development of integrated polariton circuits. A number of nonlinear effects arising from giant optical Kerr-like polariton nonlinearity, such as dark and bright solitons,[16,17] continuum generation,[18] and ultrafast pulse modulation,[19] have been reported in the WG polariton platform.

III-nitride based polaritons are of particular interest since they enable coherent emission and low threshold ultrafast nonlinear

© Author(s) 2023

optical modulation in the UV spectral range and can operate at RT[19] with many potential applications including studies of chemical reactions, coherent Raman spectroscopy, and manipulation of trapped ions. UV polariton lasing in III-nitride WG devices has been reported only recently in GaN ridge resonators up to 150 K, likely limited by the smaller exciton binding energy in bulk GaN[20] compared to that in quantum heterostructures.

In this paper, we report polariton lasing in microring resonators fabricated from GaN/AlGaN quantum well (QW) slab WGs with operation in a wide temperature range from 4 to 300 K enabled by the large exciton binding energy in the GaN QWs (~48 meV) and a lower surface state recombination velocity than their III-arsenide counterparts.[21] Polariton lasing from the multiple ring resonator modes is revealed by the threshold-like dependence of the emission intensity with increasing pump pulse energy. The free spectral range (FSR) between the modes reduces as the polariton energy approaches that of the exciton due to the strong dependence of the polariton group velocity on the photonic fraction of the polaritons, a clear signature of strong exciton–photon coupling. Furthermore, a strong blueshift of the lower polariton exciton-like states with increasing pulse energy is observed due to polariton interactions.

Apart from the development of coherent UV polariton sources, our demonstration of microring polariton resonators also paves the way toward further applications in integrated polariton circuits (e.g., filtering and directional coupling) and studies of low threshold generation of frequency combs and Kerr solitons.

Our microring resonators are formed by etching an AlGaN planar slab WG containing multiple GaN QWs,[15] which was grown by metal–organic vapor phase epitaxy on *c*-plane free-standing GaN substrate. Propagating polaritons have been demonstrated in similar unetched planar WGs with a Rabi-splitting of ~60 meV.[15] The confinement induced by the ring geometry is expected to lead to discrete clockwise and counterclockwise ring polariton modes. The samples are fabricated by means of e-beam lithography and reactive ion etching.

After etching, the total height of the structures amounts to ~315 nm [Fig. 1(a)]. Rings of different radii (R) and widths (t) have been etched on the sample. The radius is measured from the center to the mid-point of the ring. Here we studied microrings with R = 3, 4, 6, and 8 μm and t = 2 μm. A scanning electron microscopy (SEM) image of a typical microring (R = 3 μm and t = 1 μm) is shown in Fig. 1(b) (see also Fig. S1 in the supplementary material).

We study polariton lasing over a wide range of temperatures (T = 4–300 K) by using a continuous flow liquid helium cryostat. A standard microphotoluminescence (μ-PL) setup allows us to excite and collect light emission at different spots on the sample in a backscattering configuration [see Fig. 1(b)]. Pulsed laser excitation is performed with a frequency-quadrupled optical parametric amplifier (TOPAS) pumped by a Ti:sapphire regenerative amplifier. The excitation pulses were centered around 320 nm and had a duration of 100 fs and a repetition rate of 1 kHz. The PL signal collected by a microscope objective (NA = 0.39) is sent to a spectrometer with a resolution of 0.16 nm while being integrated over the entire rectangular entrance slit of the monochromator.

The optical resonances in the ring structures occur when the circumference of the ring is an integer multiple (m) of the polariton wavelength. This condition can be written as $k(E)2\pi r_{\mathrm{eff}} = 2\pi m$, where $k(E)$ is the polariton wavenumber at energy E and r_{eff} is

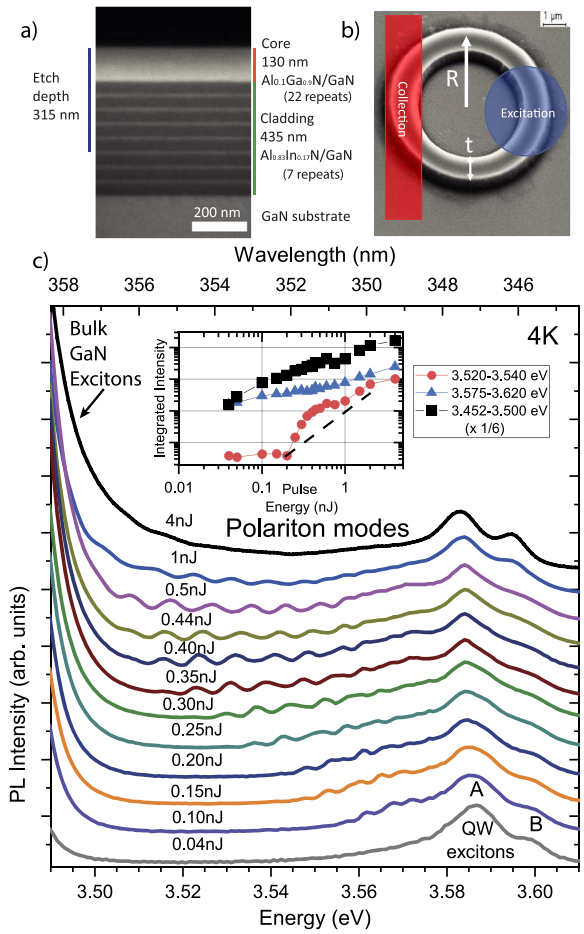

FIG. 1. (a) Cross-section scanning electron microscopy (SEM) image of the waveguide structure with relevant geometric parameters. (b) SEM image of a ring resonator at a tilted angle of 30° from the surface normal, R = 3 μm and t = 1 μm, with overlaid excitation and collection areas. (c) PL spectra (linear scale) of an AlGaN resonator with t = 2 μm and R = 4 μm collected at T = 4 K for pulse energies ranging from 0.04 to 4 nJ. The PL intensity is normalized to the intensity of the QW A exciton: the signal obtained from the exciton is divided by a different factor for each power so that it is equal to unity for all powers. The spectra are then shifted for clarity by half-unity. See also supplementary material Sec. 2. Inset: Integrated intensities (log–log scale) for the region with modes on which background contribution is negligible (red), the region corresponding to the QW exciton (blue), and the region corresponding to the bulk GaN exciton (black). The black dashed line represents a quadratic increase.

the effective radius at which the mode propagates. In addition, the finite thickness of the ring may give rise to quantization of polariton waves along the radial direction and formation of transverse modes characterized by the integer quantum number n. We calculated the optical modes of the circular waveguides using the Lumerical MODE finite difference eigenmode (FDE) solver (see supplementary material discussion 4).

To demonstrate polariton lasing, we carried out a PL pulse energy dependence study on the R = 4 μm and t = 2 μm resonator with pulse energies varying from 0.04 to 4 nJ. The emission spectra

© Author(s) 2023

for this entire excitation range at $T = 4$ K are shown in Fig. 1(c). At low pulse energies, the spectra consist of excitonic peaks at ~3.587 and ~3.598 eV associated with QW A and B excitons, as previously reported in studies led on similar wafer samples.[15] Even though the detection and excitation regions are spatially separated, exciton emission in the detection region may arise from the propagation of high velocity upper polaritons away from the excitation spot with their subsequent relaxation into the lower energy low momenta exciton states. Upon increasing pulse energy, narrow full width at half maximum (FWHM) ~3 meV modes start to appear abruptly at energies below the QW exciton peaks, first closer to the QW exciton emission, and then at lower energies down to 3.501 eV between the QW excitonic peaks and the bulk GaN exciton emission (centered at ~3.46 eV) originating from the substrate.

As we argue below, the appearance of these modes with increasing pulse energy is associated with stimulated polariton scattering into the optical ring resonator states, which are in the strong coupling regime with the QW excitons. The bulk GaN excitons are isolated from the ring structure by the cladding layers and thus are only weakly coupled to the resonator modes. Importantly, our polariton system is nonequilibrium: the multiple modes (co-existing condensates) become macroscopically occupied due to the dynamical equilibrium between gain and dissipation channels.[22,23] At 4 K, relaxation to the polariton states occurs mainly through exciton–exciton and exciton–polariton scattering, since at low temperature phonon-assisted scattering is inefficient.[24] Initially, at pulse energies just above the threshold, scattering to the exciton-like polariton states whose energy is close to the QW exciton level is more efficient. With further increase in pulse energy scattering to more photon-like states increases[25] leading to polariton lasing from the lower energy ring states [see Fig. 1(c)]. The macroscopical occupation of the polariton modes is confirmed by the superlinear (threshold-like) increase of the mode emission intensity (integrated in the energy interval where the background from GaN and QW excitons is negligible) with pulse energy, whose dependence is much faster than quadratic, as shown in the inset of Fig. 1(c). If the filling factor of the polariton modes was less than unity, it is expected that enhanced relaxation due to interparticle scattering would lead only to a quadratic dependence. For comparison, we also show in the inset of Fig. 1(c) that the integrated emission intensity exhibits a linear or slightly superlinear power dependence in the energy range where QW and GaN backgrounds dominate, respectively.

We note that in our case the modes are confined in the vertical direction due to TIR and the emission is likely observed due to Rayleigh scattering on fabrication imperfections of the ring resonators.

Below the threshold, the polariton emission from the ring resonator modes is too weak to be detected because the latter is guided in the microring resonator plane. It is only above the threshold that the scattered light from the lasing modes becomes sufficiently strong and comparable to the excitonic background to be coupled to our microscope objective.

The FSR of the ring resonator modes is given by the following equation:

$$\mathrm{FSR} = \frac{\hbar v_G(E)}{r_{\mathrm{eff}}}, \tag{1}$$

where $\hbar$ is the reduced Planck's constant and $v_G(E)$ is the (energy dependent) group velocity of planar slab WG polariton modes at energy E, and r_{eff} is the radius around which the lasing modes propagate. In the strong coupling regime $v_G(E)$ and hence the FSR is expected to decrease strongly with increasing E as the lower polariton dispersion curves strongly toward the exciton level (see supplementary material discussion 5). We investigated the stimulated emission from ring resonators of different radii at 4 K over the wavelength range 346–354 nm, with the raw data shown in Fig. 2(a). The FSR vs energy is summarized in Fig. 2(b). The FSR increases with decreasing ring radius R, as expected from Eq. (1). The FSR also decreases with increasing energy. For $R = 3$ and 4 μm, the FSR decreases drastically by a factor of 2–3 as the energy approaches the exciton level, which is a strong confirmation that the observed modes are in the strong coupling regime. Some trend of decreasing FSR with energy is also visible for $R = 6$ and 8 μm, although the dependence is more noisy for $R = 8$ μm since the FSR becomes comparable to the spectral resolution. The theoretical FSR for purely photonic modes was calculated using FDE as described above and the FSR for polaritons was calculated using the photonic values and a standard coupled oscillator model (see supplementary material Sec. 5). The solid lines in Fig. 2(b) show the theoretical polariton FSR and their curvature is in good agreement with the experiment. The purely photonic FSR theory curves (dashed lines) also show decreasing FSR with energy, which occurs mainly due to the energy dependence of the material refractive indices. However, this curvature is much shallower than that seen in the experiment. In summary, the strong curvature of the FSR vs energy cannot be explained without invoking a strong coupling picture, thus confirming that the system remains strongly coupled while in the lasing regime. Further detail is given in the supplementary material Sec. 5.

Furthermore, we perform measurements on an $R = 8$ μm microring over a wider temperature range up to 300 K. The PL spectra for different pulse energies are displayed in Figs. 3(a)–3(c) for $T = 4$, 200 and 300 K, respectively. At all temperatures, the bunch of narrow ring resonator modes associated with polariton lasing appear below the QW A exciton energy level with increasing pulse energy. As in the case of $R = 4$ μm, the emission intensities integrated in the energy range where modes are the most visible demonstrate a clear threshold-like behavior with a faster than quadratic dependence in Figs. 3(d)–3(f) at all temperatures, indicating macroscopic occupation and lasing of several modes. By contrast, the bulk GaN and QW excitonic peaks behave linearly (see supplementary material Sec. 7). As the data taken at 200 and 300 K sits on a strong incoherent PL background originating from the bulk GaN and the QW exciton emission peaks, this background has been subtracted. The resulting PL spectra are available in the supplementary material (Sec. 6). In the supplementary material (Sec. 5), we plot FSR measurements at 300 K and compare them with the theoretical simulations, which support the strong exciton–photon coupling at room temperature.

While with increasing temperature both the exciton and the polariton emission shift to lower energy due to bandgap reduction, it is also observed that the onset of lasing occurs in more photon-like polariton states at higher T. This occurs because (a) the losses of the exciton-like states with energies closer to the exciton level increase due to phonon scattering, and (b) at elevated temperature, the polaritons can relax to more photon-like states by exciton–phonon

© Author(s) 2023

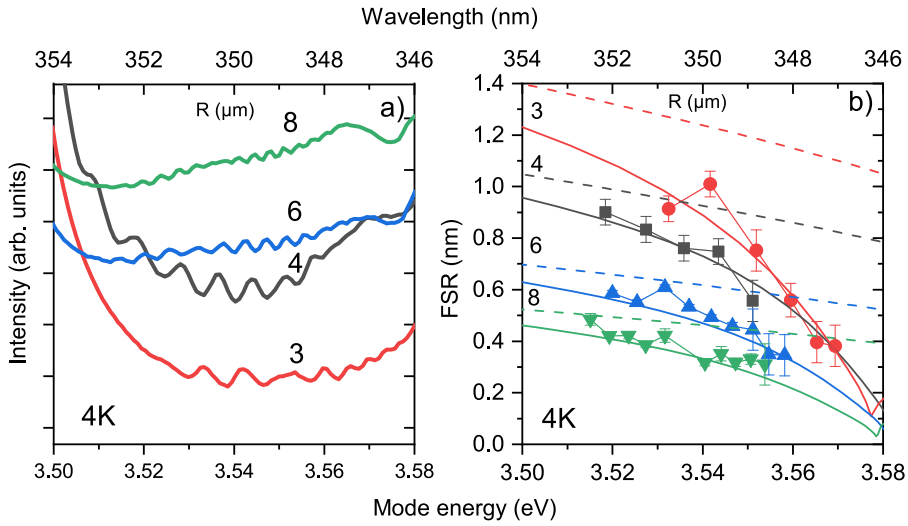

FIG. 2. (a) PL spectra in a linear scale of microring resonators measured for different radii (3, 4, 6, and 8 μm), with a 2 μm width, at pulse energy above threshold (0.4 nJ) taken at 4 K. (b) Free spectral range of the same rings. The solid lines are a fit according to Eq. (1) accounting for the excitonic content of the guided modes. The dashed lines show the results of a purely photonic model. Simulation details and FSR data recorded at 300 K are shown in the supplementary material (Secs. 4 and 5).

as well as exciton–exciton and exciton–polariton scattering.[24–26] The non-radiative processes and polariton losses increasing with temperature also lead to the increase of the lasing threshold from 0.25 nJ at 4 K to 0.35 nJ and ~1.8 nJ at 200 and 300 K, respectively. Interestingly, however, this overall increase in the polariton lasing threshold with temperature remains within a factor of about seven. Such a variation is far smaller than that reported recently for ridge waveguide polariton lasers made from bulk GaN, where the drastic increase in the lasing threshold by more than two orders of magnitude from 70 to 220 K was incompatible with a polaritonic picture that could hold from cryogenic to room temperature.[20] This reduced sensitivity for our sample is again most likely stemming from the quantum heterostructure nature of our polariton gain medium, which leads to stabler excitons. We are also able to explore a significant range of pumping conditions above the threshold with pulse energy values nearly up to an order of magnitude larger than those at the threshold at 4 K for the 8 μm ring resonator [Figs. 3(d)–3(f)] and even beyond one order of magnitude for the 4 μm ring resonator [Fig. 1(c) and corresponding inset].

The excitonic component of the polariton wavefunction leads to strong polariton–polariton interactions responsible for the blueshift of polariton resonances with increasing density. In

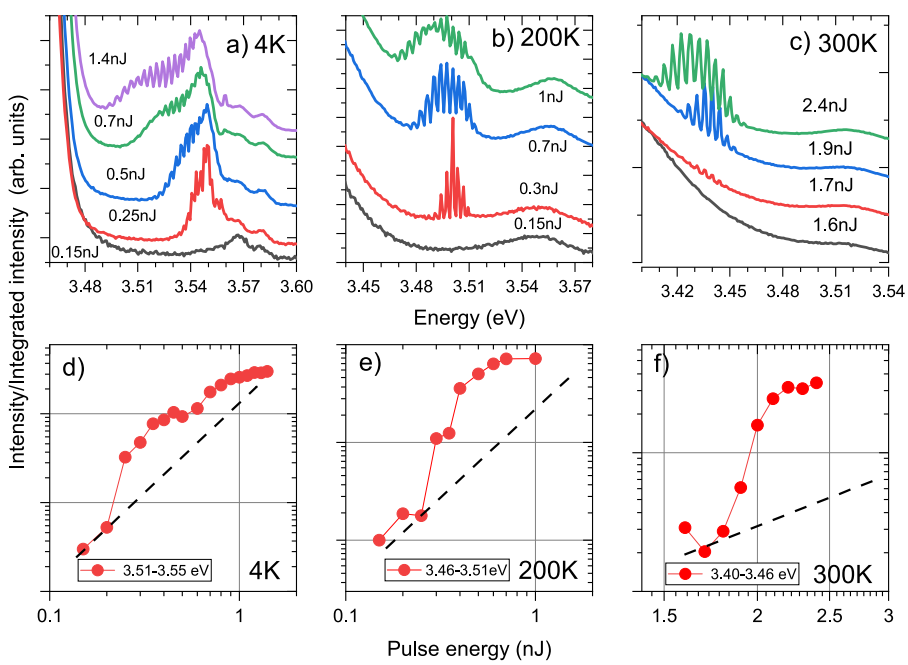

FIG. 3. (a)–(c) PL spectra for the 8 μm radius, 2 μm wide ring at different pulse energies (in nJ) labeled in the figures for T = 4, 200, and 300 K, respectively. Each spectrum is normalized to the QW A exciton (3.566 eV at 4 K, 3.547 eV at 200 K, and 3.511 eV at 300 K) and then shifted for clarity. Non-shifted values and an alternative presentation are given in supplementary material Sec. 2. (d)–(f) Integrated intensity of the modes within given energy boundaries plotted in log–log scale for T = 4, 200, and 300 K, respectively. The black dashed line represents a quadratic increase.

© Author(s) 2023

Figs. 4(a)–4(c), we plot expanded spectra for different pulse energies, tracing the peak position of each of the lasing modes. The extracted peak positions of the polariton modes are plotted in Figs. 4(d)–4(f), respectively. As expected, the higher energy exciton-like states exhibit a stronger blueshift with pulse energy than the lower energy photon-like polaritons. At 4 and 200 K, an energy blueshift up to 6–7 meV is observed for exciton-like modes, with the excitonic fraction ranging from 0.91 to 0.24 for 4 K and from 0.57 to 0.21 at 200 K, whereas at 300 K the observed shifts are much less, ~1 – 2 meV, due to the decreased excitonic content of the lasing modes, ranging this time from 0.20 to 0.08, and increased thermal effects, which may lead to a polariton redshift counterbalancing the effect of interactions. Note that only inter- and intra-mode polariton–polariton interactions are responsible for the polariton blueshifts, whereas the interaction with the higher energy exciton reservoir does not play a role since its density is expected to be pinned above the polariton lasing threshold.[27] The evolution of the peak intensity of the modes with pulse energy is finally given in Figs. 4(g)–4(i). The peak intensity is given by the maximum intensity of the mode minus the intensity at the base of the peak. We can see that the modes examined here have a different threshold-like increase at a given pulse energy, and then stagnate or decrease as

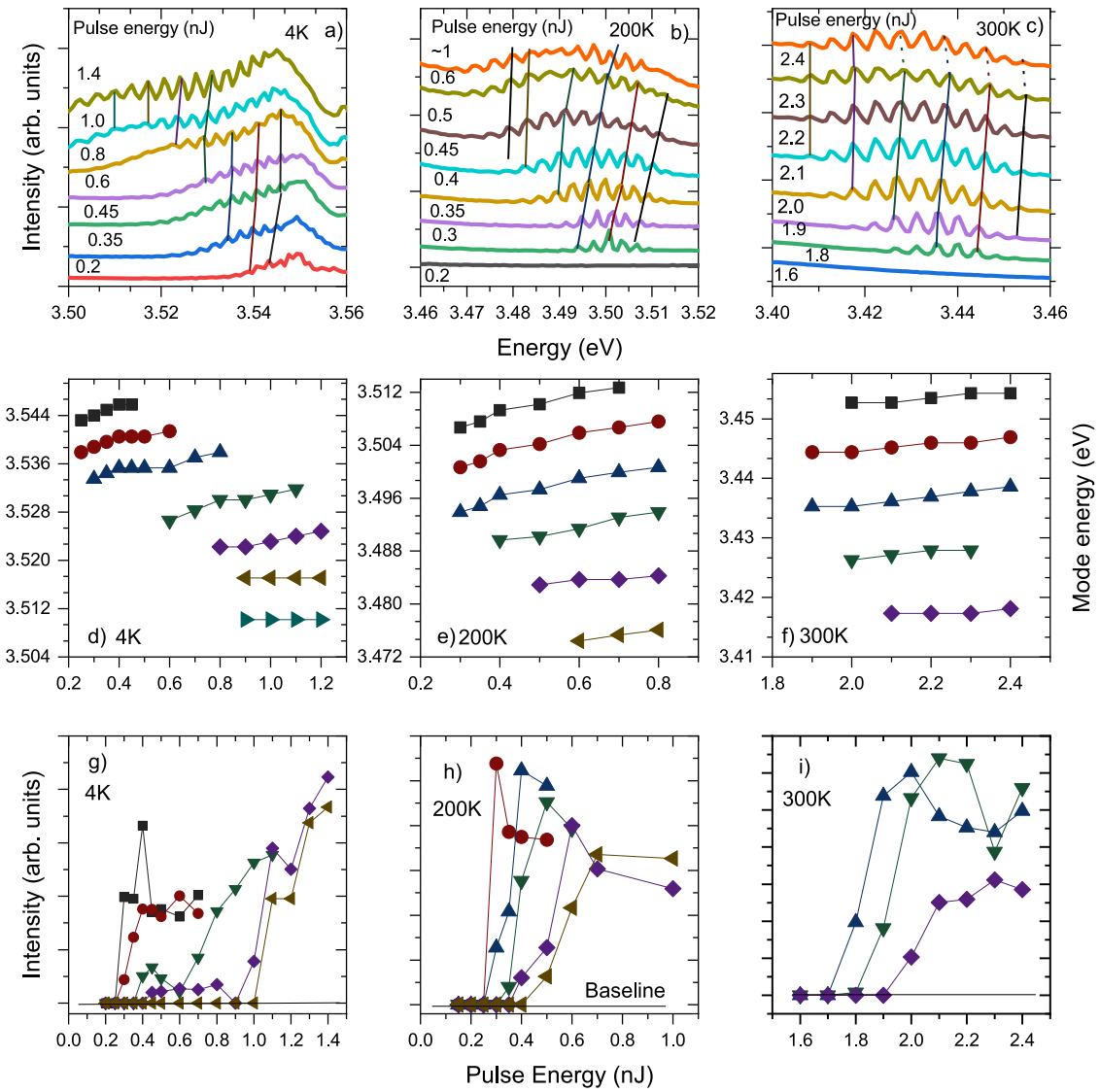

FIG. 4. (a)–(c) PL spectra of the 8 μm ring resonator taken at T = 4, 200, and 300 K, respectively. The solid lines act as guides for the eye to indicate the shift of selected modes with pulse energy. The dashed lines represent points where the shift is less visible. Data are obtained from Fig. 3. (d)–(f) Mode energy vs pulse energy of selected modes, identified by the line color, at 4, 200, and 300 K, respectively. (g)–(i) The peak mode intensity vs pulse energy of selected polariton modes, identified by their line color, at 4, 200, and 300 K, respectively.

© Author(s) 2023

more modes, and hence mode competition, come into play. Similar strong blueshifts are seen in the 4 μm ring at 4 K (see supplementary material Sec. 8). Finally, we note that interparticle interactions and mode competition may determine the linewidth (FWHM ~ 2–3 meV) of the lasing modes above threshold (see supplementary material Sec. 3).

Importantly, the fact that the exciton emission line, detected either in the area of the pump spot or on the opposite side of the ring (Figs. 1 and 3), does *not* broaden with pulse energy and shows no or small energy blueshift (~10 meV) confirms that there is a limited screening of the built-in electric field and that the created electron–hole density in each QW is well below the Mott density (~10^{12} cm^{-2}).[28] Indeed, above the Mott density, the emission is expected to originate from an electron–hole plasma with a high energy emission tail extending by 50–60 meV from the exciton peak maxima.[28] This observation is another confirmation that the nonlinear emission is associated with polariton lasing.

In conclusion, we report UV polariton lasing from multiple modes in microring resonators fabricated from AlGaN planar waveguides with embedded GaN quantum wells at temperatures up to 300 K. The micro-structured polariton system we present has the potential to be used to study modelocking of polaritons into a sequence of short pulses, generation of UV soliton trains, and frequency combs supported by giant polariton Kerr nonlinearity. Polariton modelocking was demonstrated numerically for resonantly pumped microring resonators.[29] Beyond this, a non-resonant pump like the one used in this work and a combination of both resonant and non-resonant pumping offer several avenues for further research into the complex interplay between turbulence and modelocking.[30] Additional opportunities should arise from the coupling between two and more rings, which includes combining space topology and modelocking,[31] an aspect not easily within reach with the linear WG geometry. Overall, our work has the potential to be a significant step forward for the development of compact active nonlinear polariton devices operating at RT.

See supplemental document for supplementary material concerning experimental methods and simulation models for polariton dispersion.

We acknowledge the UK EPSRC Grant Nos. EP/V026496/1, EP/S030751/1, and EP/R007977/1. Anthonin Delphan would like to thank Christopher Vickers and Thomas Ball for their help with the cryogenics setup.

AUTHOR DECLARATIONS

Conflict of Interest

The authors have no conflicts to disclose.

Author Contributions

Anthonin Delphan: Conceptualization (equal); Data curation (equal); Formal analysis (equal); Investigation (equal); Methodology (equal); Software (equal); Validation (equal); Visualization (equal); Writing – original draft (equal). **Maxim N. Makhonin**: Conceptualization (equal); Data curation (equal); Formal analysis (lead); Investigation (equal); Methodology (equal); Software (lead); Supervision (equal); Validation (equal); Visualization (equal); Writing – original draft (lead). **Tommi Isoniemi**: Investigation (equal); Methodology (equal); Resources (equal); Writing – review & editing (supporting). **Paul M. Walker**: Conceptualization (equal); Data curation (equal); Formal analysis (equal); Methodology (equal); Software (equal); Visualization (equal); Writing – review & editing (lead). **Maurice S. Skolnick**: Conceptualization (equal); Methodology (equal); Writing – review & editing (supporting). **Dmitry N. Krizhanovskii**: Conceptualization (equal); Funding acquisition (lead); Methodology (equal); Project administration (lead); Supervision (equal); Writing – review & editing (lead). **Dmitry V. Skryabin**: Methodology (equal); Writing – review & editing (supporting). **Jean-François Carlin**: Methodology (equal); Resources (equal); Writing – review & editing (supporting). **Nicolas Grandjean**: Methodology (equal); Resources (equal); Writing – review & editing (supporting). **Raphaël Butté**: Conceptualization (equal); Methodology (equal); Project administration (equal); Supervision (equal); Writing – review & editing (lead).

DATA AVAILABILITY

The data that support the findings of this study are available from the corresponding author upon reasonable request.

REFERENCES

[1] J. Kasprzak, M. Richard, S. Kundermann, A. Baas, P. Jeambrun, J. M. J. Keeling, F. M. Marchetti, M. H. Szymańska, R. André, J. L. Staehli, V. Savona, P. B. Littlewood, B. Deveaud, and L. S. Dang, Nature **443**, 409 (2006).
[2] D. Bajoni, P. Senellart, E. Wertz, I. Sagnes, A. Miard, A. Lemaître, and J. Bloch, Phys. Rev. Lett. **100**, 047401 (2008).
[3] A. Amo, J. Lefrère, S. Pigeon, C. Adrados, C. Ciuti, I. Carusotto, R. Houdré, E. Giacobino, and A. Bramati, Nat. Phys. **5**, 805 (2009).
[4] M. Sich, D. V. Skryabin, and D. N. Krizhanovskii, C. R. Phys. **17**, 908 (2016).
[5] A. Delteil, T. Fink, A. Schade, S. Höfling, C. Schneider, and A. İmamoğlu, Nat. Mater. **18**, 219 (2019).
[6] T. Kuriakose, P. M. Walker, T. Dowling, O. Kyriienko, I. A. Shelykh, P. St-Jean, N. C. Zambon, A. Lemaître, I. Sagnes, L. Legratiet, A. Harouri, S. Ravets, M. S. Skolnick, A. Amo, J. Bloch, and D. N. Krizhanovskii, Nat. Photonics **16**, 566 (2022).
[7] A. Amo and J. Bloch, C. R. Phys. **17**, 934 (2016).
[8] S. Ghosh and T. C. H. Liew, npj Quantum Inf. **6**, 16 (2020).
[9] A. Imamoğlu, R. J. Ram, S. Pau, and Y. Yamamoto, Phys. Rev. A **53**, 4250 (1996).
[10] S. Christopoulos, G. B. H. von Högersthal, A. J. D. Grundy, P. G. Lagoudakis, A. V. Kavokin, J. J. Baumberg, G. Christmann, R. Butté, E. Feltin, J.-F. Carlin, and N. Grandjean, Phys. Rev. Lett. **98**, 126405 (2007).
[11] C. Schneider, A. Rahimi-Iman, N. Y. Kim, J. Fischer, I. G. Savenko, M. Amthor, M. Lermer, A. Wolf, L. Worschech, V. D. Kulakovskii, I. A. Shelykh, M. Kamp, S. Reitzenstein, A. Forchel, Y. Yamamoto, and S. Höfling, Nature **497**, 348 (2013).
[12] F. Li, L. Orosz, O. Kamoun, S. Bouchoule, C. Brimont, P. Disseix, T. Guillet, X. Lafosse, M. Leroux, J. Leymarie, G. Malpuech, M. Mexis, M. Mihailovic, G. Patriarche, F. Réveret, D. Solnyshkov, and J. Zuniga-Perez, Appl. Phys. Lett. **102**, 051102 (2013).
[13] G. Christmann, R. Butté, E. Feltin, J.-F. Carlin, and N. Grandjean, Appl. Phys. Lett. **93**, 051102 (2008).
[14] P. M. Walker, L. Tinkler, M. Durska, D. M. Whittaker, I. J. Luxmoore, B. Royall, D. N. Krizhanovskii, M. S. Skolnick, I. Farrer, and D. A. Ritchie, Appl. Phys. Lett. **102**, 012109 (2013).

© Author(s) 2023

[15] J. Ciers, J. Roch, J.-F. Carlin, G. Jacopin, R. Butté, and N. Grandjean, Phys. Rev. Appl. **7**, 034019 (2017).
[16] P. M. Walker, L. Tinkler, D. V. Skryabin, A. Yulin, B. Royall, I. Farrer, D. A. Ritchie, M. S. Skolnick, and D. N. Krizhanovskii, Nat. Commun. **6**, 8317 (2015).
[17] P. Walker, L. Tinkler, B. Royall, D. Skryabin, I. Farrer, D. Ritchie, M. Skolnick, and D. Krizhanovskii, Phys. Rev. Lett. **119**, 097403 (2017).
[18] P. M. Walker, C. E. Whittaker, D. V. Skryabin, E. Cancellieri, B. Royall, M. Sich, I. Farrer, D. A. Ritchie, M. S. Skolnick, and D. N. Krizhanovskii, Light: Sci. Appl. **8**, 6 (2019).
[19] D. M. Di Paola, P. M. Walker, R. P. A. Emmanuele, A. V. Yulin, J. Ciers, Z. Zaidi, J.-F. Carlin, N. Grandjean, I. Shelykh, M. S. Skolnick, R. Butté, and D. N. Krizhanovskii, Nat. Commun. **12**, 3504 (2021).
[20] H. Souissi, M. Gromovyi, T. Gueye, C. Brimont, L. Doyennette, D. Solnyshkov, G. Malpuech, E. Cambril, S. Bouchoule, B. Alloing, S. Rennesson, F. Semond, J. Zúñiga-Pérez, and T. Guillet, Phys. Rev. Appl. **18**, 044029 (2022).
[21] M. Boroditsky, I. Gontijo, M. Jackson, R. Vrijen, E. Yablonovitch, T. Krauss, C.-C. Cheng, A. Scherer, R. Bhat, and M. Krames, J. Appl. Phys. **87**, 3497 (2000).
[22] J. Kasprzak, D. D. Solnyshkov, R. André, L. S. Dang, and G. Malpuech, Phys. Rev. Lett. **101**, 146404 (2008).
[23] D. N. Krizhanovskii, K. G. Lagoudakis, M. Wouters, B. Pietka, R. A. Bradley, K. Guda, D. M. Whittaker, M. S. Skolnick, B. Deveaud-Plédran, M. Richard, R. André, and L. S. Dang, Phys. Rev. B **80**, 045317 (2009).
[24] J. Ciers, D. D. Solnyshkov, G. Callsen, Y. Kuang, J.-F. Carlin, G. Malpuech, R. Butté, and N. Grandjean, Phys. Rev. B **102**, 155304 (2020).
[25] A. I. Tartakovskii, M. Emam-Ismail, R. M. Stevenson, M. S. Skolnick, V. N. Astratov, D. M. Whittaker, J. J. Baumberg, and J. S. Roberts, Phys. Rev. B **62**, R2283 (2000).
[26] P. G. Savvidis, J. J. Baumberg, D. Porras, D. M. Whittaker, M. S. Skolnick, and J. S. Roberts, Phys. Rev. B **65**, 073309 (2002).
[27] M. Wouters and I. Carusotto, Phys. Rev. Lett. **99**, 140402 (2007).
[28] G. Rossbach, J. Levrat, G. Jacopin, M. Shahmohammadi, J.-F. Carlin, J.-D. Ganière, R. Butté, B. Deveaud, and N. Grandjean, Phys. Rev. B **90**, 201308(R) (2014).
[29] O. A. Egorov and D. V. Skryabin, Opt. Express **26**, 24003 (2018).
[30] M. Piccardo, B. Schwarz, D. Kazakov, M. Beiser, N. Opačak, Y. Wang, S. Jha, J. Hillbrand, M. Tamagnone, W. T. Chen, A. Y. Zhu, L. L. Columbo, A. Belyanin, and F. Capasso, Nature **582**, 360 (2020).
[31] Z. Yang, E. Lustig, G. Harari, Y. Plotnik, Y. Lumer, M. A. Bandres, and M. Segev, Phys. Rev. X **10**, 011059 (2020).

© Author(s) 2023